Article

Cell Reports

Selective Maturation of Temporal Dynamics of Intracortical Excitatory Transmission at the Critical Period Onset

Graphical Abstract

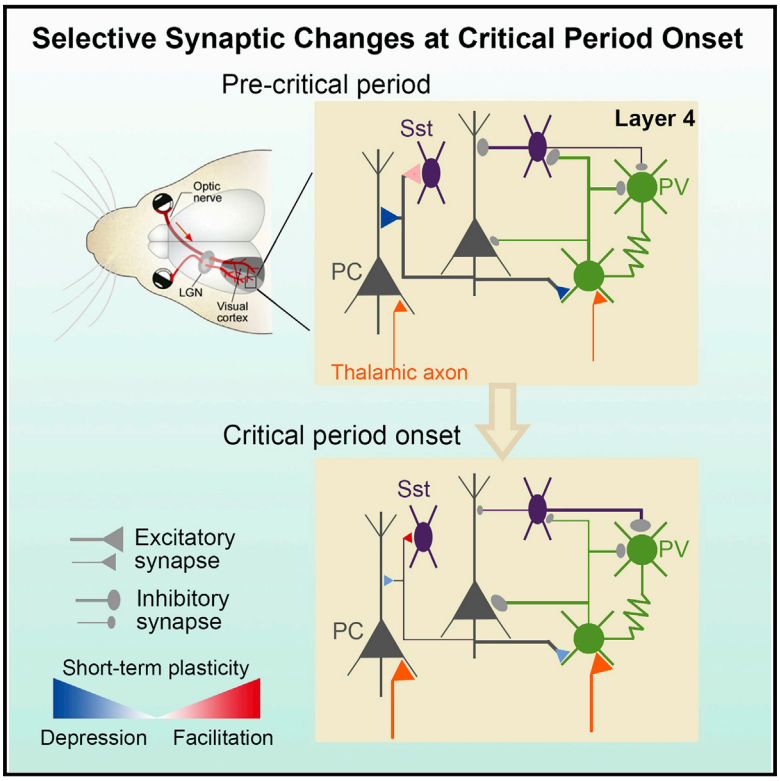

Highlights

- Temporal dynamics of intracortical excitatory synapses mature at critical period onset
- Dynamics of cortical inhibitory synapses and thalamocortical inputs are unchanged
- This selective modulation depends on early visual experience
- Ubiquitous reduction of presynaptic release underlies the selective modulation.

Authors

Qinglong Miao, Li Yao, Malte J. Rasch, Qian Ye, Xiang Li, Xiaohui Zhang

Correspondence

xhzhang@bnu.edu.cn

In Brief

Miao et al. demonstrate that in the developing visual cortical layer 4 circuit, temporal dynamics of intracortical excitatory synapses are selectively regulated by visual experience prior to the critical period onset. This provides an additional essential circuit mechanism for regulating critical period plasticity aside from the well-known inhibitory threshold mechanism.

Miao et al., 2016, Cell Reports *16*, 1–13
August 16, 2016
http://dx.doi.org/10.1016/j.celrep.2016.07.013

CellPress

Please cite this article in press as: Miao et al., Selective Maturation of Temporal Dynamics of Intracortical Excitatory Transmission at the Critical Period Onset, Cell Reports (2016), http://dx.doi.org/10.1016/j.celrep.2016.07.013

Cell Reports
Article

Selective Maturation of Temporal Dynamics of Intracortical Excitatory Transmission at the Critical Period Onset

Qinglong Miao,[1,2,3] Li Yao,[1,3] Malte J. Rasch,[1] Qian Ye,[1] Xiang Li,[1] and Xiaohui Zhang[1,*]
[1]State Key Laboratory of Cognitive Neuroscience and Learning, IDG/McGovern Institute for Brain Research, Beijing Normal University, Beijing 100875, China
[2]Institute of Neuroscience, Shanghai Institutes for Biological Sciences, University of Chinese Academy of Sciences, Chinese Academy of Sciences, Shanghai 200031, China
[3]Co-first author
*Correspondence: xhzhang@bnu.edu.cn
http://dx.doi.org/10.1016/j.celrep.2016.07.013

SUMMARY

Although the developmental maturation of cortical inhibitory synapses is known to be a critical factor in gating the onset of critical period (CP) for experience-dependent cortical plasticity, how synaptic transmission dynamics of other cortical synapses are regulated during the transition to CP remains unknown. Here, by systematically examining various intracortical synapses within layer 4 of the mouse visual cortex, we demonstrate that synaptic temporal dynamics of intracortical excitatory synapses on principal cells (PCs) and inhibitory parvalbumin- or somatostatin-expressing cells are selectively regulated before the CP onset, whereas those of intracortical inhibitory synapses and long-range thalamocortical excitatory synapses remain unchanged. This selective maturation of synaptic dynamics results from a ubiquitous reduction of presynaptic release and is dependent on visual experience. These findings provide an additional essential circuit mechanism for regulating CP timing in the developing visual cortex.

INTRODUCTION

Neuronal circuits in many brain regions are functionally immature at birth. Their synaptic wiring and function undergo experience-dependent maturation postnatally, which is especially heightened during well-defined early postnatal time windows, namely critical periods (CPs) (Hubel and Wiesel, 1970; Levelt and Hübener, 2012). The experience-dependent plasticity during the CP is best exemplified by visual input-dependent ocular dominance (OD) plasticity in the developing mammalian primary visual cortex (V1), which is essential for the emergence of the binocular vision (Wang et al., 2010; Espinosa and Stryker, 2012). An evolution of patterned cortical activities during early development has been proposed to play critical roles in initiating the CP (Toyoizumi et al., 2013; Chen et al., 2015). Temporal patterns of neuronal spiking activity are important for inducing structural plasticity of dendritic spines (Wyatt et al., 2012) that underlies the CP plasticity (Mataga et al., 2004). Dynamic changes of synaptic efficacy in the context of patterned spike trains, also known as short-term synaptic plasticity (STP), are critical elements that are involved in the dynamic processing of neural information in a neural circuit (Klug et al., 2012; Klyachko and Stevens, 2006). Previous studies showed that transgenic mice that lacked experience-dependent CP plasticity often exhibited defects in STP at some cortical synapses (Choi et al., 2002; Postma et al., 2011; Gu et al., 2013; He et al., 2014). Specifically, deletion of *gad 65* (the 65-kDa isoform of glutamic acid decarboxylase GAD65) or *Cx36* (connexin36, a gap junction protein) resulted in an absence of the CP plasticity and impaired STP at GABAergic synapses in response to high-frequency activations in the visual cortical circuit (Hensch et al., 1998; Choi et al., 2002; Postma et al., 2011). Moreover, selective deficiency of neuronal activity-regulated pentraxin (NARP) or Rett syndrome-related protein methyl-CpG-binding protein 2 (MeCP2) in parvalbumin (PV)-expressing GABAergic interneurons also impaired the STP at cortical excitatory synapses onto PV cells and the CP plasticity in the developing mouse V1 (Gu et al., 2013; He et al., 2014). These findings suggest that synaptic dynamics at cortical excitatory and inhibitory synapses could be involved in the regulation of CP plasticity of developing V1 circuits.

In addition to receiving afferent inputs from various subcortical areas, excitatory and inhibitory neurons in the sensory neocortex construct an intricate neural network by forming diverse synapses among them. Intracortical excitatory and inhibitory synapses, which are actively involved in dynamic transfer and processing of synaptic information (Abbott and Regehr, 2004; Etherington and Williams, 2011; Rotman et al., 2011; Klug et al., 2012), exhibit differential STP properties (Thomson, 1997; Markram et al., 1998; Reyes et al., 1998; Gupta et al., 2000; Beierlein and Connors, 2002; Beierlein et al., 2003; Ma et al., 2012). Moreover, the STP of neocortical synapses, which is modulated by experience developmentally (Takesian et al., 2010; Lu et al., 2014), could contribute to the regulation of CP

Please cite this article in press as: Miao et al., Selective Maturation of Temporal Dynamics of Intracortical Excitatory Transmission at the Critical Period Onset, Cell Reports (2016), http://dx.doi.org/10.1016/j.celrep.2016.07.013

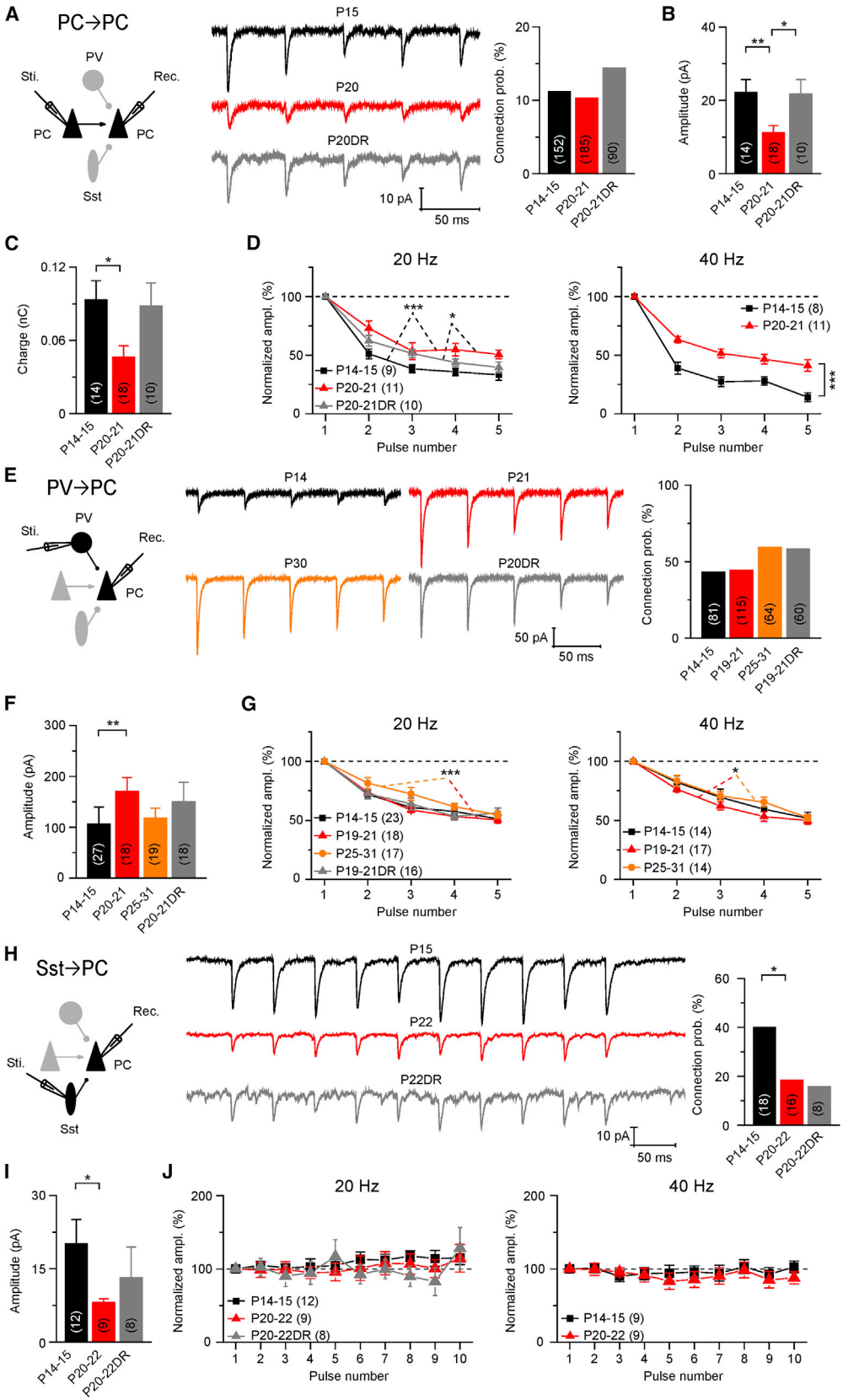

(legend on next page)

plasticity of the developing V1 (Choi et al., 2002; Postma et al., 2011; Gu et al., 2013; He et al., 2014). However, given the diverse synapses with differential STP properties in neocortical circuits, a systematic examination on developmental regulation of the dynamics of diverse cortical synapses during the transition to CP is still lacking.

In the present study, using whole-cell recordings in acute mouse visual cortical slices, we systematically examined the developmental changes of STP of the intracortical synapses among excitatory principal cell (PC), inhibitory PV-, and somatostatin (Sst)-expressing interneuron as well as the afferent thalamocortical excitatory synapse onto the layer 4 PC and PV interneuron during a period from eye opening (postnatal days 14–15 [P14–15]) to the CP onset (P19–21). Our results show that STP of intracortical excitatory synapses, but neither intracortical inhibitory synapses nor long-range thalamocortical synapses, undergo differential changes during the transition to CP. Dark rearing of animals from birth prevents the developmental modulation of STP at the intracortical excitatory synapses, suggesting the requirement of visual experience during the process. Further variance-mean analyses of synaptic transmission reveal that a ubiquitous reduction of presynaptic glutamate release probability underlies the selective STP modulation at developing intracortical excitatory synapses. Thus, our results demonstrate a synaptic mechanism by which intracortical excitatory synapses in the developing V1 layer 4 circuits contribute to the transition to CP.

RESULTS

Developmental Modulation of STP at Intracortical Synapses onto Layer 4 PCs Is Restricted to Excitatory Synapse

The CP for OD plasticity in the developing mouse V1 begins at P19–20 and peaks at P28–30 (Gordon and Stryker, 1996). To examine developmental changes of synaptic dynamics at cortical synapses across the CP, we systematically assayed transmission strength and dynamics of synapses within the cortical layer 4, a main thalamorecipient lamina. Acute slices of visual cortex were prepared from mice at different postnatal ages, as follows: immediately after eye opening (P14–15, pre-CP), at the CP onset (P19–21), and during the CP (P25–31). In the first set of experiments, we examined intracortical excitatory and inhibitory synapses onto PC. By recording from pairs of layer 4 PCs (Figure 1A), we found that connection probability between PCs (PC→PC synapse) was 11.2% (17 connections out of 152 tested pairs) and 10.3% (19 connections out of 185 tested pairs) for pre-CP (P14–15) and CP onset (P19–21), respectively (Figure 1A, right; $p = 0.79$, χ^2 test). However, despite of the constant connection probability, the amplitude and total charge of basal unitary PC→PC excitatory postsynaptic currents (uEPSCs) decreased by 49.6% and 50.3%, respectively, from P14–15 to P20–21 (Figures 1B and 1C). This result is consistent with a recent study on layer 2/3 recurrent excitatory synapses in the developing mouse V1 (Ko et al., 2013), but different from the observed increase of PC-PC synaptic strength in the developing rat layer 4 circuit (Wang et al., 2012). This discrepancy could result from different species. Moreover, the average uEPSC 10%–90% rise and decay time remained unchanged (Table S1). However, PC→PC synaptic transmission showed a significant decrease in short-term depression (STD), elicited by five consecutive presynaptic pulses at 20 Hz, from P14–15 to P20–21 (Figures 1A and 1D; $p = 1.8 \times 10^{-6}$, two-way ANOVA), and this reduction was more significant when 40 Hz pulses were used ($p = 5.2 \times 10^{-12}$).

The transition from pre-CP to CP depends on experience. To examine whether the developmental changes at the PC→PC synapse observed above depend on experience, we dark-reared mice from birth, which is known to effectively delay the opening of CP (Espinosa and Stryker, 2012). We found that the unitary EPSC amplitude, total charge, and STD properties at PC→PC synapses in dark-reared mice were similar to that of P14–15 mice (Figures 1B–1D), suggesting experience dependence of the developmental modulations from pre-CP to the CP onset.

We next examined whether similar developmental changes may occur at intracortical inhibitory synapses during the same period. GABAergic inhibitory interneurons can be classified into distinct subgroups based on the expression of different calcium-binding proteins and neuropeptides, among which PV- and Sst-expressing neurons constitute a large fraction (Markram et al., 2004; Xu et al., 2010; Rudy et al., 2011). In this set of experiments, inhibitory PV and Sst cells were labeled with tdTomato by respectively crossing *PV-Cre* and *Sst-Cre* transgenic mice to the Cre-dependent tdTomato reporter mice *Ai9* (see Experimental Procedures).

Simultaneous recordings were made on pairs of PV cell and PC in the layer 4 in slices prepared from P14–15, 19–21, and 25–31 mice. We found that, while inhibitory synapse from PV cell onto PC (PV→PC) showed little change in its connection probability (Figure 1E, right; $p > 0.05$ for all two-group comparisons, χ^2 test), its uEPSC amplitudes increased by 60.4% from P14–15 to P19–21 (Figures 1E, middle, and 1F). However, the STD of PV→PC inhibitory synapse did not change from the pre-CP to CP onset when tested with 5 consecutive presynaptic pulses at 20 or 40 Hz (Figure 1G) or with 10 pulses at 20 Hz (Figures S1A and 1B). Dark-rearing until P20–21 did not affect the unitary strength and STD of PV→PC inhibitory synapses (Figures 1F and 1G), suggesting that the developmental change at

Figure 1. Selective Modulation of STP of Intracortical Synapses onto Layer 4 PC at the Transition to CP

(A) Left: diagram for paired whole-cell recordings of excitatory PC→PC synapse. Middle: representative traces of averaged uEPSCs recorded (Rec.) from a PC in slices from P15, P20, or P20DR mice. Right: connection probability at different postnatal stages.

(B and C) Summarize results of average amplitude (B) and total charge (C) of the first uEPSCs.

(D) STDs of PC→PC synapses, tested by presynaptic stimuli at 20 (left) and 40 Hz (right), at P14–15, P20–21, and P20–21DR.

(E–G) Similar to (A)–(D), except at the PV→PC inhibitory synapse.

(H–J) Similar to (A)–(D), except at the Sst→PC inhibitory synapses.

Error bars in the plots represent SEM. *$p < 0.05$, **$p < 0.01$, ***$p < 0.001$. n, the number of tested synapses.

Please cite this article in press as: Miao et al., Selective Maturation of Temporal Dynamics of Intracortical Excitatory Transmission at the Critical Period Onset, Cell Reports (2016), http://dx.doi.org/10.1016/j.celrep.2016.07.013

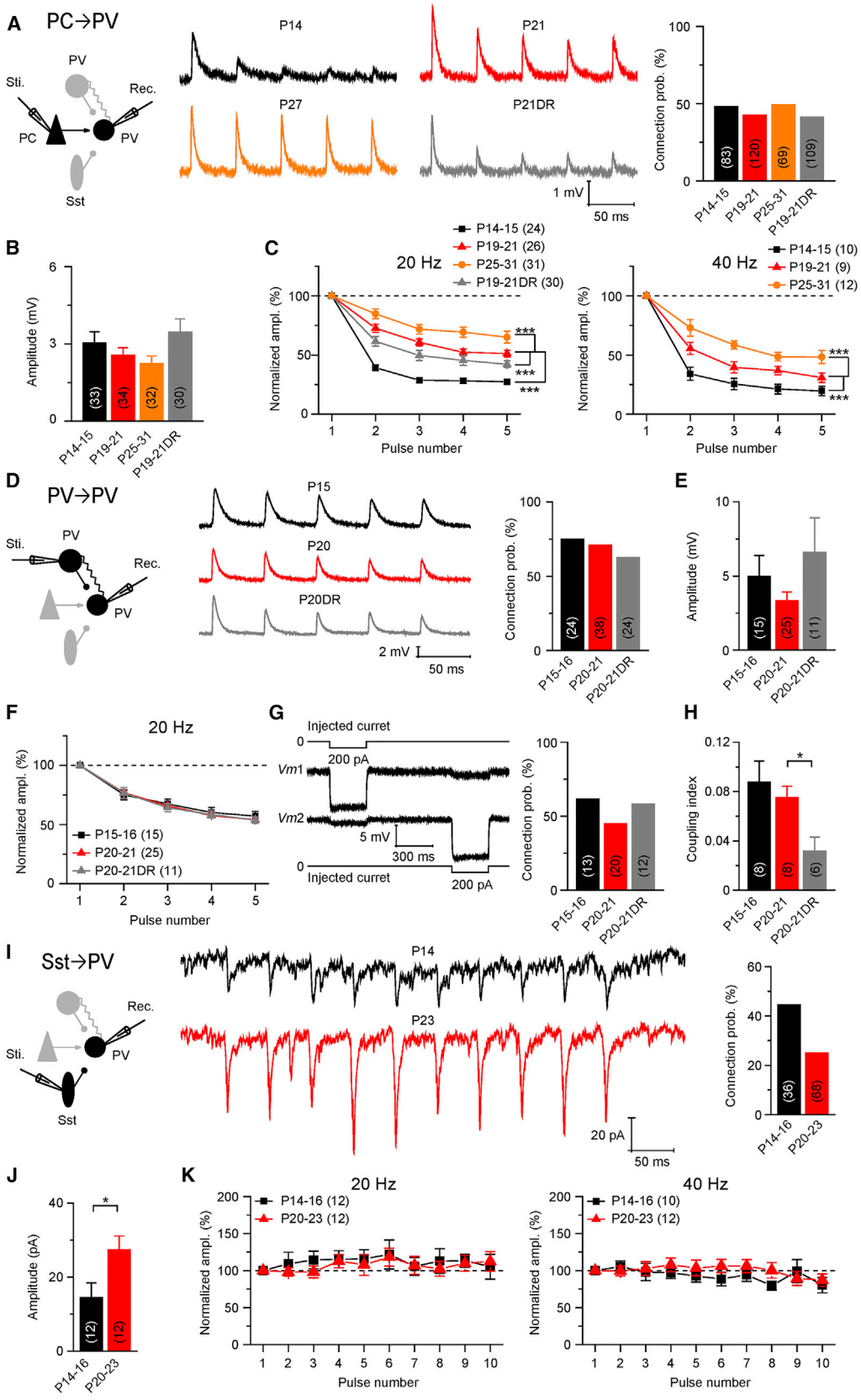

(legend on next page)

PV-PC inhibitory synapses is independent on experience. In contrast, there was a slight but significant decrease in the STD of PV→PC synapse during the CP (Figure 1G; p = 0.00053, P19–21 versus P25–31, ANOVA; Figures S1A and S1B).

Sst cells are another major subgroup of inhibitory interneuron, comprising approximately 30% of all neocortical interneurons (Rudy et al., 2011) and forming inhibitory synapses primarily on distal dendrites of the PC (Fino and Yuste, 2011). In visual cortical slices from *Sst-Cre::Ai9* mice, we used a train of 10 presynaptic spikes at 20 or 40 Hz to assay the efficacy and STP of layer 4 Sst→PC inhibitory synapses due to their relatively low release probability (Figure 1H). Unlike the PC→PC and PV→PC synapses that show STD, Sst→PC synapse in the layer 4 exhibited a slight short-term facilitation (STF) (Figure 1H). We found that the connection probability between the Sst cell and PC decreased substantially from P14–15 to P20–22 (p = 0.0071, χ^2 test; Figure 1H, right), along with decreased average strength (Figure 1I). However, no change was observed in the STF of Sst→PC inhibitory synapses from P14–15 to P20–22 when tested at 20 or 40 Hz (Figure 1J; p = 0.14 for 20 Hz; p = 0.22 for 40 Hz; ANOVA). Moreover, dark rearing had no effect on the connection probability, unitary strength, or STF at Sst→PC inhibitory synapses over this developmental period (Figures 1H–1J).

Taken together, these results suggest that within the layer 4, excitatory and inhibitory synapses onto the PC undergo differential functional changes during the transition to CP onset, while experience-dependent selective modulation of STP occurs only at the PC→PC excitatory synapse.

Differential STP Changes at Intracortical Synapses onto Inhibitory PV Cells

Given that PV-mediated cortical inhibition is considered as a key factor in regulating the CP onset (Hensch, 2004; Espinosa and Stryker, 2012), we next examined local afferent synapses onto layer 4 PV cells during the transition to CP. Because the membrane resistance (R_m) of cortical PV cells was low and developmentally reduced (P14–15, 78.50 ± 3.80 MΩ, n = 34; P19–21, 56.64 ± 1.72 MΩ, n = 44), unitary postsynaptic synaptic potentials (uPSPs), rather than unitary PSCs, were recorded from the PV cell under the current-clamp mode (see Experimental Procedures). Our recordings showed that the PC→PV connection probability did not change from P14 to P30 (Figure 2A; p > 0.05, χ^2 test). Although the average uEPSP amplitude of the PC→PV synapse did not change significantly across these developmental periods (Figure 2B), its STDs, tested by 20 or 40 Hz presynaptic pulses, were significantly attenuated (Figures 2A, traces, and 2C; ANOVA). Similar changes in STDs at these PC→PV excitatory synapses were also observed over the development when uEPSCs were measured under voltage-clamp (Figures S1C–S1F). We also noted that the uEPSP kinetics became faster over the development (Table S1). Moreover, dark rearing of mice until P19–21 retarded the developmental attenuation of STD of PC→PV excitatory synapses (p = 0.0002, P21 dark-reared [DR] versus P21, AONVA), while its connection probability and unitary strength were not affected (Figures 2A–2C, gray color). Collectively, the developmental attenuation of STD of PC→PV excitatory synapses, together with the increased reciprocal PV→PC inhibitory strength (Figure 1F), at the CP onset can lead to an enhanced feed-back cortical inhibition exerted by PV cells.

Both chemical and electrical synapses exist between neighboring cortical PV cells to form an inhibitory network (Pangratz-Fuehrer and Hestrin, 2011). We next examined these two types of synapse onto layer 4 PV cells, with simultaneous whole-cell recordings from neighboring PV cells in the V1 slices at P15–16 and P20–21. The probabilities of forming GABAergic chemical synapses between two PV cells were 75% and 71% at P15–16 and P20–21, respectively (Figure 2D; p = 0.73, χ^2 test), and ~50% of the tested pairs showed reciprocal chemical synapses at both ages (P15–16, 54.5%; P20–21, 52.6%). The averaged amplitude of unitary inhibitory postsynaptic potential (uIPSP) remained largely unchanged from the pre-CP to CP onset (Figure 2E), but there was a substantial reduction of its rise and decay time (Table S1). However, unlike the PC→PV excitatory synapse, PV→PV inhibitory synapse did not show any developmental change in STD from pre-CP to CP onset when tested with 20 Hz presynaptic spikes (Figures 2D and 2F; p = 0.15, ANOVA). We also observed that the couple probability and efficacy of electrical synapse between PV cells were not changed during the transition to the CP onset (Figures 2G and 2H). Moreover, dark rearing largely unaffected both chemical and electrical synapses between the PV cells except for decreasing the electrical coupling efficacy (Figures 2D, 2E, 2G, and 2H, gray; p = 0.027 in Figure 2H).

In the cortical inhibitory network, PV cells also receive inhibitory afferents from the Sst cell within the same layer, forming a dis-inhibitory circuit (Gibson et al., 1999; Pfeffer et al., 2013; Xu et al., 2013). Thus, we further examined the development of layer 4 Sst→PV inhibitory synapse in visual cortical slices from *Sst-Cre::Ai9* mice at P14–16 and P20–23 (Figure 2I, left). Our results showed that (1) its connection probability decreased during the transition to the CP onset (p = 0.043, χ^2 test; Figure 2I, right) and (2) its average uIPSC amplitude

Figure 2. Distinct Modulation of STP of Intracortical Synapses onto Inhibitory PV Cells

(A) Left: diagram for paired whole-cell recordings of PC→PV inhibitory synapses. Middle: representative traces of averaged uEPSPs recorded (Rec.) from a PV cell in slices from P14, P21, P27, or P21DR mice. Right: connection probability at different postnatal stages.

(B) Summarized results of the average amplitude of the first uEPSPs.

(C) STDs of PC→PV excitatory synapse, tested with five presynaptic spikes at 20 (left) and 40 Hz (right), at P14–15, P19–21, P25–31, and P19–21DR.

(D–F) Similar to (A)–(C), except at PV→PV inhibitory synapses.

(G) Left: representative traces of membrane potential deflection recorded from a PV cell (Vm1), induced by current injection (200 pA; 300 ms) in another PV cell (Vm2), and vice versa. Right: connection probability of electrical connections between two PV cells at different postnatal stages.

(H) Summarized coupling index of electrical synapses at P15–16, P20–21, and P20–21DR.

(I–K) Similar to (A)–(C), except at Sst→PV inhibitory synapse.

Error bars represent SEM. *p < 0.05, ***p < 0.001. n, the number of tested synapses.

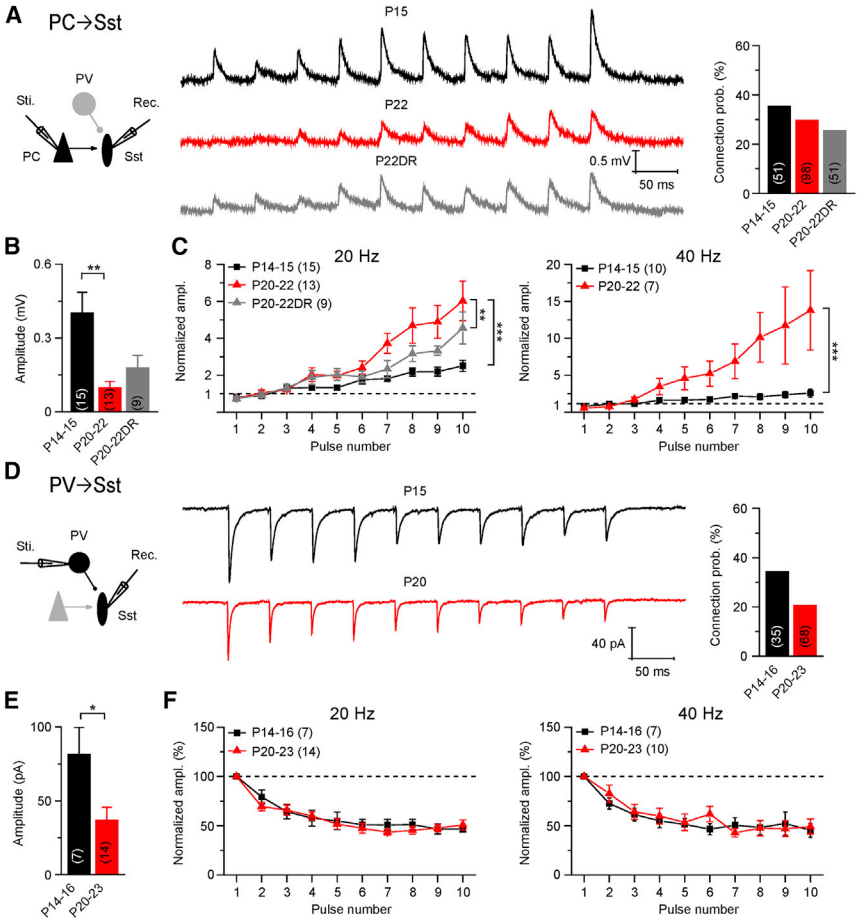

Figure 3. Developmental Change of STP of Intracortical Synapses onto Sst Cells

(A) Left: diagram for paired whole-cell recordings of PC→Sst excitatory synapses. Middle: representative traces of averaged uEPSPs recorded (Rec.) from a Sst cell in slices from P15, P22, and P22DR mice. Right: connection probability at different postnatal stages.

(B) Summarized results of average amplitude of the first uEPSPs.

(C) STFs of PC→Sst synapse, tested by 10 presynaptic spikes at 20 (left) or 40 Hz (right), at P14–16, P20–22, and P20–22DR.

(D–F) Similar to (A)–(C), except at PV→Sst inhibitory synapses. Error bars represent SEM. *$p < 0.05$, **$p < 0.01$, ***$p < 0.001$. n, the number of tested synapses.

increased by 89.7% (p = 0.005, Figure 2J), along with decreased rise time and τ_{decay} of uIPSCs (Table S1). When tested with 20 or 40 Hz presynaptic pluses, Sst→PV inhibitory synapses showed neither depression nor facilitation, and there was no change in STP from the pre-CP to CP onset (Figures 2I, middle, and 2K; p = 0.39 and 0.096 for 20 and 40 Hz, ANOVA).

Thus, by examining diverse types of local synapse onto the PV cell, we again demonstrate that only STP at intracortical excitatory synapses onto the PV cell undergoes an experience-dependent modulation from the pre-CP to CP onset.

STP Change in Inhibitory Sst Cells Is Also Confined to Excitatory Synapses

We further examined the developmental modulation of local synapses onto the layer 4 Sst cell. The PC→Sst excitatory synapse has characteristically low release probability and strong STF (Reyes et al., 1998; Rozov and Burnashev, 1999). Indeed, we observed a strong STF at the PC→Sst excitatory synapse when 10 presynaptic pulses at 20 or 40 Hz were delivered (Figure 3A). To calculate the extent of STF, each unitary excitatory postsynaptic potential (uEPSP) amplitude was normalized to the mean amplitude of the first 3 uEPSPs. We found that while the probability of forming PC→Sst synapses changed little from the pre-CP to CP onset (p = 0.48, χ^2 test; Figure 3A), their unitary strength was greatly reduced (measured by the average amplitude of the first uEPSPs, p = 0.0032; Figure 3B). Moreover, there was no significant change in the uEPSP kinetics (Table S1). Interestingly, the PC→Sst excitatory synapse exhibited an augmentation in STF from P14–15 to P20–22 ($p = 4.8 \times 10^{-11}$, 20 Hz; $p = 1.1 \times 10^{-7}$, 40 Hz; AONVA; Figures 3A and 3C). Further experiments using dark-reared mice at P20–22 showed that visual deprivation effectively retarded the developmental augmentation of STF at the PC→Sst synapse, while its connection probability and unitary strength were not affected (Figures 3A–3C).

Cortical Sst cells barely form inhibitory synapse between themselves (Gibson et al., 1999; Hu et al., 2011), but receive inhibitory synapses from other types of cortical interneurons including the PV cell (Ma et al., 2012; Pfeffer et al., 2013). For layer 4 PV→Sst inhibitory synapses, we found 12 connected pairs out of 35 tested (34.3%) at P14–16 and 14 connected pairs out of 68 tested (20.6%) at P20–23, indicating little change in its connection probability during this developmental period (p = 0.13, χ^2 test; Figure 3D), while their unitary strength decreased by 54.9% (Figure 3E). Similarly, STP of the PV→Sst inhibitory synapses also showed no change from the pre-CP to CP onset (p = 0.38, 20 Hz; p = 0.45, 40 Hz; ANOVA; Figures 3D and 3F). However, the uIPSCs showed significant changes in their kinetics over this period (Table S1).

Taken all above results together, our systematic examination on different intracortical synapses formed among layer 4 PC, PV, and Sst cells suggests that STP of local excitatory synapses from the PC is selectively modulated in a target-cell-independent manner from eye opening to the CP onset. In contrast, STPs of all local inhibitory synapses are kept constant, despite changes in the connection probability, strength, and response kinetics among various intracortical synapses.

Unchanged STP of Thalamocortical Synapses onto Layer 4 PC and PV Cells

Given that visual thalamic inputs directly project to the layer 4 PC and PV cell (Cruikshank et al., 2010; Kloc and Maffei, 2014), we also examined these long-range thalamocortical (tc) excitatory synapses. To isolate putative tcEPSPs recorded from PCs or PV cells in cortical slices, a cortical silencing cocktail (50 μM muscimol and 70 μM SCH50911) was applied in the artificial cerebrospinal fluid (aCSF) bath solution (Liu et al., 2007; Khibnik et al., 2010). A concentric bipolar electrode (diameter 125 μm) was placed at the white matter to activate the ascending axonal fibers, which consist of both TC projection axons and thinner cortical collateral fibers from the layer 6 corticothalamic (CT) cells (Figure 4A). Consistent with previous results (Ahmed et al., 1997; Beierlein and Connors, 2002), the field stimulation often elicited the following two components of monosynaptic EPSPs in the layer 4 PCs and PV cells: tcEPSPs with short latencies and corticothalamic (ct)EPSPs with relatively longer latencies (Figures 4A–4C2). Such separation of the TC and CT inputs was further confirmed by analyzing the ratio of latencies of the first two EPSPs (second/first) (Beierlein and Connors, 2002), in which ctEPSPs showed a systematic decrease in the latency ratio ($p = 0.007$, nonparametric paired-sample sign test; Figure 4D, bottom) and tcEPSPs did not ($p = 0.69$; Figure 4D, top). Moreover, ctEPSPs were less STD than tcEPSPs in the PC and PV cell (Figures 4B1 and 4B2). We used these criteria to separate the evoked tcEPSPs in the following analysis.

We first assessed developmental changes of the strength of TC inputs (tcEPSPs) in the layer 4 PC or PV cell in slices prepared from P15–16 or P20–21 mice, by increasing stimulation intensity stepwise to achieve the maximal amplitude of the first tcEPSP (see Experimental Procedures). The results showed an elevated input/output curves for the TC excitatory inputs to both PCs (TC→PC) (Figure 4E, $p = 0.032$; Kolmogorov-Smirnov test) and PV cells (TC→PV) (Figure 4F, top; $p = 0.0034$) over this period. Similar to previous results from the somatosensory and visual cortices (Cruikshank et al., 2010), tcEPSPs evoked by 20 Hz spike trains in the PV cell were more easily depressed than that in the PC (Figures 4B1, 4B2, 4E, and 4F). However, when comparing the STD between P15–16 and P20–21, we did not observe any significant difference at the TC→PC and TC→PV synapses between these two ages (Figures 4E and 4F, bottom; $p = 0.27$ and 0.23 for TC→PC and TC→PV synapses, ANOVA). It suggests that, unlike the layer 4 intracortical excitatory synapses, the temporal dynamics of these long-range TC excitatory inputs are not developmentally modulated from pre-CP to CP onset.

Ubiquitous Decrease in Presynaptic Release Probability at Intracortical Excitatory Synapses

Next, we examined presynaptic or postsynaptic mechanisms that underlie the selective modulation of STPs of the intracortical excitatory synapses over the development. Analysis of the failure rate and the coefficients of variation (C.V.) of evoked synaptic responses at individual PC→PC, PC→PV, and PC→Sst excitatory synapses indicated that the theses two parameters significantly increased from P14–15 to P19–22 (Figure 5A), implicating a developmental reduction of presynaptic release probability at these excitatory synapses. The presynaptic change was further tested by performing the variance-mean (V-M) analysis of uEPSCs/uEPSPs to directly estimate the number of release sites (N), the presynaptic release probability (Pr), and the postsynaptic quantal size (Q), which are three major variables determining the quantal release efficacy (Scheuss and Neher, 2001; Gu et al., 2013). As shown by an example PC→PV excitatory synapse, parabola fit of the mean versus variance of amplitudes of individual uEPSPs was made, and then the binomial equation yielded the estimated values of N, Pr, and Q of this PC→PV synapse (Figure 5B). Implementation of the same estimation to all layer 4 PC→PC, PC→PV, and PC→Sst excitatory synapses examined at P14–15 and P20–22 revealed a ubiquitous reduction of Pr and unchanged N and Q at all three synapses (Table S2). We further validate the V-M analysis results by another experiment of altering extracellular [Ca^{2+}] (Mitra et al., 2012) at 1, 2, and 3.7mM for the PC→PV excitatory synapse at P14–15 and obtained similar N and Pr values (Pr: 0.66 ± 0.025; N: 8.56 ± 1.89; Q: 21.75 ± 1.58 pA; n = 5). Thus, developmental reduction of Pr is a common presynaptic factor involved in the selective modulation of STPs at all examined intracortical excitatory synapses in the layer 4 circuit.

Activity-dependent relief from the polyamine block of postsynaptic Ca^{2+}-permeable (CP) α-amino-3-hydroxy-5-methyl-4-isoxazolepropionic acid (AMPA) receptors (CP-AMPARs) can act as a postsynaptic mechanism underlying the STP regulation at cortical PC→PV excitatory synapses (Rozov and Burnashev, 1999). To determine whether this postsynaptic mechanism may contribute to the observed selective developmental modulation of STP at layer 4 PC→PV excitatory synapses, we measured its STP at P14 and P21 using an internal solution supplemented with 50 μM spermine. The effectiveness of spermine blockage on CP-AMPARs was confirmed by measuring the inward-rectification of AMPAR-mediated EPSCs in the PC or PV cell (Figure S2A, in the presence of 50 μM D-AP5 and 50 μM picrotoxin), and only the PV cell showed characteristic inwardly rectifying current-voltage (I-V) plots (Figures S2B and S2C). We then examined the STP of PC→PV synapse using the spermine-containing internal solution and found that the STD showed similar attenuation from eye opening to the CP onset (Figures S2D and S2E) in comparison with the STD curves assayed using the normal internal solutions (Figure 2C or Figure S2E, gray lines). These results exclude a possibility that the polyamine-dependent postsynaptic signaling could account for the developmental attenuation of STD at this synapse. We also tested the effects of a selective CP-AMPAR antagonist, 1-naphthyl acetyl spermine (NAS, 100 μM in the bath), on the basal transmission and STP of the PC→PV synapse, using the normal internal solution. The results showed that 10 min after applying NAS in the bath, amplitudes of the first uEPSP were significantly reduced (Figures S2F and S2G), but there were no significant differences in the STD curves before and after the NAS application at P14–16 ($p = 0.85$) and at P20–23 ($p = 0.06$; Figure S2H). These results are in agreement with the recent finding that NAS decreased unitary synaptic responses but had little effect on STD of layer 2/3 PC→PV synapses in mouse V1 around P20 (Lu et al., 2014). However, when comparing the STD curves measured under the NAS application (blue lines in Figure S2H) between P14–16 and P20–23, it still

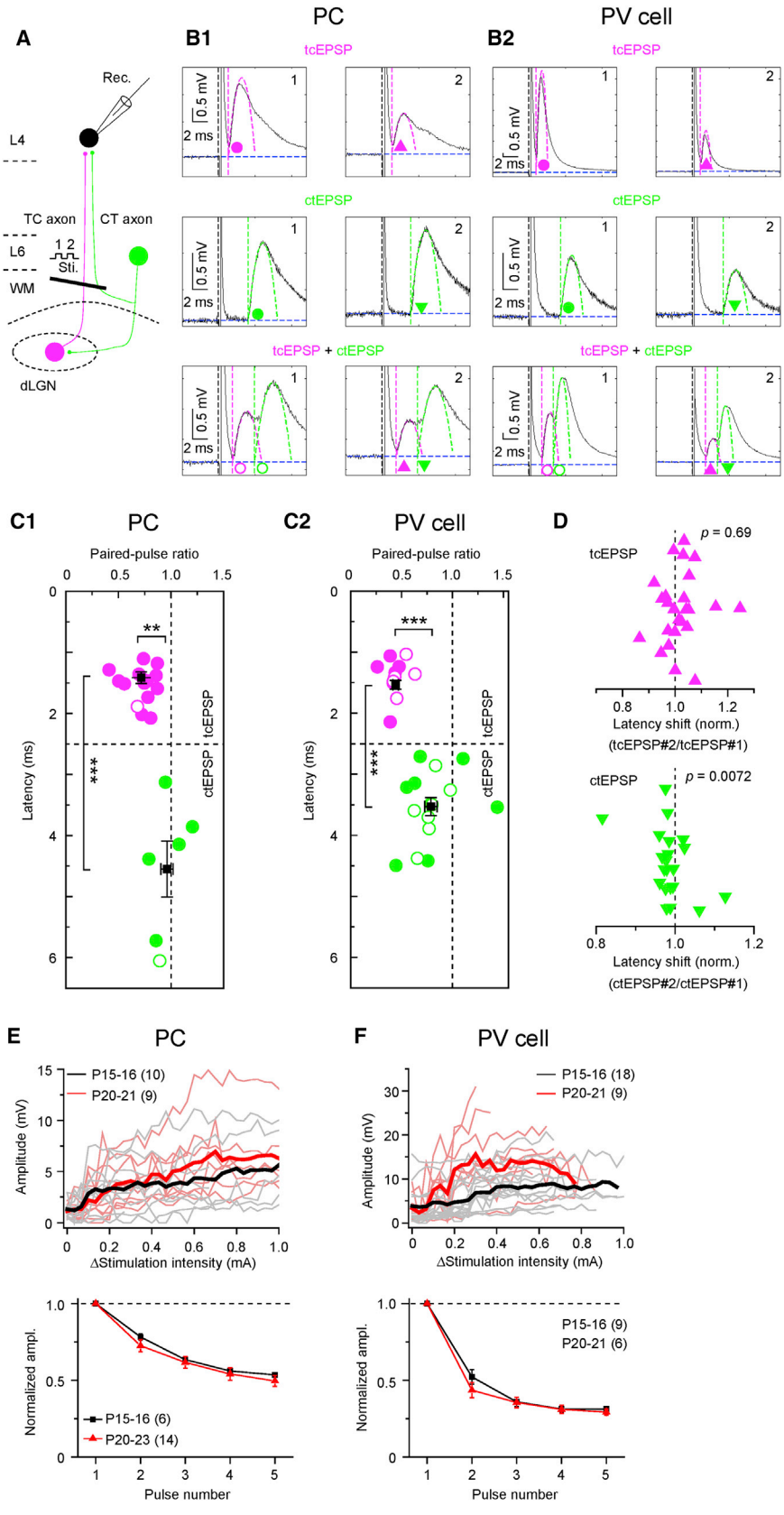

Figure 4. Unchanged STP of Long-Range TC Synapses onto Layer 4 PC and PV Cells during the Transition to CP

(A) Schematic diagram depicting the field electrical stimulation (Sti.) activation of thalamocortical (TC) and corticothalamic (CT) axons and the recording (Rec.) of synaptic currents from the layer 4 (L4) neuron. WM, white matter; dLGN, dorsal lateral geniculate nucleus.

(B1 and B2) Two distinct components of EPSPs recorded from the PC (B1) or PV cell (B2) in the presence of cortical silencing cocktail (50 μM muscimol and 70 μM SCH509911). Rows: putative tcEPSPs (top) showing paired-pulse depression and short latencies (magenta closed circles), ctEPSPs (middle) exhibiting less paired pulse depression and longer latencies (green closed circles), and the combined responses (tcEPSP + ctEPSP, bottom) (magenta and green open circles). Note the onset time of tcEPSPs (magenta vertical dashed line) and ctEPSPs (green vertical dashed line) are determined by the intersection of the baseline (horizontal dashed line) with a parabola fit to the rising phase of tcEPSP and ctEPSP, respectively.

(C1 and C2) Correlation plots of the latency time and the paired-pulse ratio for evoked EPSPs recorded from the PC (C1; n = 18) and PV cell (C2; n = 18), respectively. Horizontal dashed lines denote the boundary (latency 2.5 ms) for separating tcEPSP and ctEPSP. Squares with error bars: mean values of the latency and the paired-pulse ratio (±SEM).

(D) Plots of the latency ratio of the second EPSP to the first one. Note that the ratios for tcEPSPs (n = 25) center to 1, while that for ctEPSPs (n = 21) bias toward <1.

(E) Top: input-output curves of the Δstimulation intensity (above the threshold value) versus the peak amplitude of tcEPSPs in the PC at P15–16 (black) and P20–21 (red). Light colored lines denote data from individual cells, and thick lines are the average curves. Bottom: comparing STDs at the TC→PC synapses between P15–16 and P20–21.

(F) Similar to (E) except the tcEPSPs in the PV cell. Error bars represent SEM. **p < 0.01, ***p < 0.001. n, the number of examined cells.

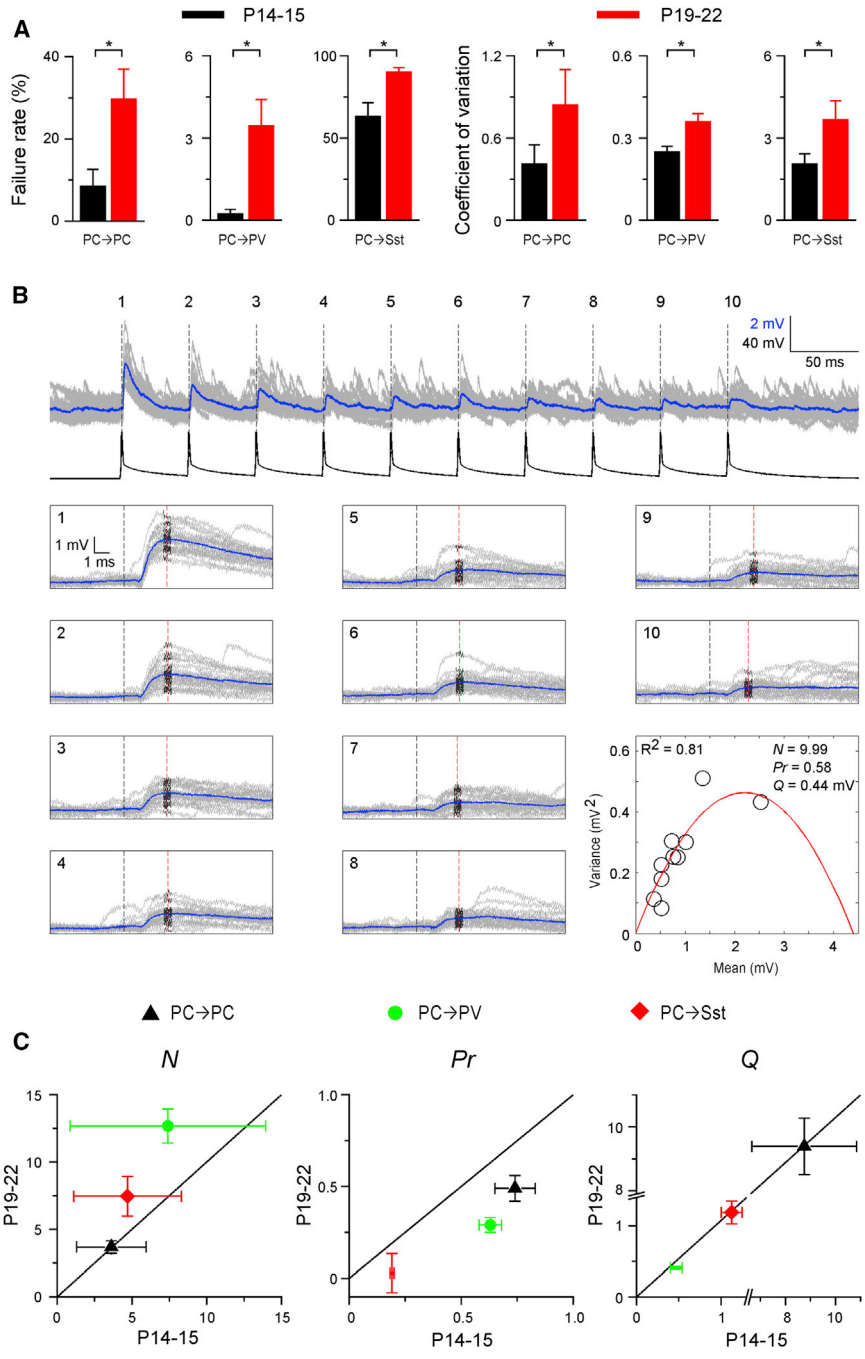

Figure 5. Ubiquitous Reduction of Presynaptic Release Probability of Intracortical Excitatory Synapses over the Development

(A) Changes of the failure rate and the coefficient of variation at the PC→PC, PC→PV, and PC→Sst excitatory synapse from P14–15 to P19–22.

(B) Individual uEPSPs (gray traces) and the averaged uEPSP (blue) recorded from a PV cell. Boxes: higher-resolution uEPSP traces in 0.5 ms windows (black), in reference to the time of averaged uEPSP peak (red dash lines), were used for detecting amplitudes of individual uEPSPs. Bottom right: a parabola fit (red line) plot of the variance and the mean of uEPSPs.

(C) Comparisons of the estimated number of release site (*N*), release probability (*Pr*), and quantal size (*Q*) of the PC→PC (black triangles), PC→PV (green circles), and PC→SST (red diamonds) excitatory synapses between P14–15 and P19–22, respectively.

Error bars represent SEM; *p < 0.05.

remained significant different (p = 0.006, comparing blue curves P14–16 versus P20–23). Thus, these results suggest that the polyamine/CP-AMPAR-dependent postsynaptic mechanism is unlikely to contribute to the developmental modulation of STP at the layer 4 PC→PV synapse during the transition to CP onset.

DISCUSSION

In this study, we found that, in the layer 4 of developing V1, STPs of intracortical excitatory synapses from PC to PC or to inhibitory PV and Sst cells are selectively regulated during the transition from pre-CP to CP. In contrast, STPs of intracortical inhibitory synapses and long-range TC excitatory synapses are not modulated during the same period. Such selective modulation at intracortical excitatory synapses results from a ubiquitous downregulation of glutamate release probability at the presynaptic PC axonal terminals targeting onto both excitatory and inhibitory cells. These systematic characterization results demonstrate that there exists a STP modulation at distinct cortical synapses in the layer 4 circuit from eye opening to the CP onset. Together with a recent study that reported selective STP modulation at cortical layer 2/3 excitatory synapses onto the PV cell during the CP (P18–30) (Lu et al., 2014), our findings suggest that distinct developmental modulations of STPs at intracortical excitatory synapses may contribute to the emergence of experience-dependent CP plasticity in the developing V1.

It has been widely accepted that the developmental enhancement of cortical inhibition primarily mediated by PV cells gates the opening of CP (Hensch, 2005). The present study could provide a circuit basis for the emergence of enhanced PV cell-mediated inhibition at the CP onset in the developing V1 layer 4. First, we showed that from pre-CP to CP onset, intracortical excitatory drive onto the PV cell becomes less depressed in response to repetitive activation in the circuit (Figures 2A–2C). In addition, the long-range excitatory TC inputs onto the PV cell is strengthened (Figure 4F). Second, the PV→PC inhibitory

Please cite this article in press as: Miao et al., Selective Maturation of Temporal Dynamics of Intracortical Excitatory Transmission at the Critical Period Onset, Cell Reports (2016), http://dx.doi.org/10.1016/j.celrep.2016.07.013

synapse, mediating the feed-forward or feed-back inhibition (Pouille and Scanziani, 2001), increases its strength during this period (Figures 1E and 1F; see Chattopadhyaya et al., 2004; Jiang et al., 2010). These two developmental changes in synaptic functions of the PV cell can contribute to the enhancement of PV cell inhibition on the PC. In contrast, both the excitatory drive onto the Sst cell (Figures 3A and 3B) and its inhibitory output (Figures 1H and 1J) are substantially reduced during the same period. These changes are expected to attenuate the Sst cell impact onto the PC activity. Thus, in the layer 4 circuit, respective levels of the inhibitions mediated by PV and Sst cells undergo opposite changes during the transition to CP onset.

In addition to forming inhibitory synapses onto the PC, GABAergic interneurons themselves are also interconnected and formed dis-inhibitory synapses (Pfeffer et al., 2013). Our results show that the Sst→PV inhibitory synapse is strengthened in the layer 4, while the reciprocal PV→Sst inhibitory synapse is conversely weakened. Such differential modulations on the dis-inhibitory synapses could counterbalance the opposite changes of the PV- and Sst cell-mediated inhibitions onto the PC when these two types of interneuron are activated simultaneously. It may also play a role in maintaining a proper excitation-inhibition (E-I) balance when the PV cell inhibition is leveled up to trigger the CP. The developmental or activity-dependent differential changes in the PV- and Sst-cell inhibitory circuits have also been found across different developing sensory cortices (Maffei et al., 2004; Bartley et al., 2008; Takesian et al., 2010, 2013). A recent study demonstrated that a delicate control of cortical PV cell inhibition via the dis-inhibitory synapse was actively involved in initiating the CP plasticity of the developing V1 (Kuhlman et al., 2013). Considering the fact of ~40% connection probability between cortical PV and Sst cells in the V1 layer 4 (Figure 3), potential roles of the Sst cell in regulating the cortical inhibition level and the CP plasticity cannot be ignored. It is of interest to elucidate whether and how the dis-inhibitory circuit plays a role in regulating the CP plasticity.

Our major finding that experience-dependent developmental modulation of STPs during the transition to CP is restricted to the intracortical excitatory synapse in the layer 4 circuit is consistent with previous electron microscopy results (Blue and Parnavelas, 1983). It reported that the number of transmitter vesicles per excitatory synaptic terminal was nearly doubled in the rat V1 from P14 (eye opening) to P28 (the CP peak), while the change at the inhibitory synaptic terminals was less than 20% during the same period (Blue and Parnavelas, 1983). A recent study also suggested that the rate of excitatory synapse maturation is highly linked to the duration of CP windows (Clement et al., 2013). Moreover, two developmental disease mouse models that lacked the CP plasticity consistently show selective defects in the intracortical excitatory synapses (Gu et al., 2013; He et al., 2014). Thus, these experimental findings also implicate that selective maturation of cortical excitatory synapses could be another important factor for regulating the E-I balance and the CP, in addition to developmental maturation of cortical inhibitory transmission, during the cortical development.

In regard to the mechanism underlying the short-term dynamics changes at the layer 4 intracortical excitatory synapses, we demonstrate that there is a ubiquitous reduction of presynaptic release probability from the pre-CP to CP onset. In particular at the neocortical PC→PV excitatory synapse, results from our study using spermine and NAS (Figure S2) and a recent study (Lu et al., 2014) both suggest that a well-known polyamine/CP-AMPAR postsynaptic mechanism (Rozov and Burnashev, 1999) is not actively involved in the modulation of STP before P20 (at the CP onset). However, this postsynaptic mechanism could make a strong contribution to STP regulation of at neocortical PC→PV synapses in later developmental stages (>P30) (Lu et al., 2014). The molecular mechanisms by which these excitatory synapses are globally modulated at presynaptic sites needs to be further examined. Several presynaptic mechanisms might be involved, such as downregulation of presynaptic NMDARs (Corlew et al., 2007; Larsen et al., 2011), progressive increase in tonic mGluR activity accompanied with decreased glutamate transporter activity (Chen and Roper, 2004), or developmental modulation of the presynaptic P/Q or N-type calcium channels (Leal et al., 2012).

Visual functions of excitatory PC, inhibitory PV, and Sst cells in the developing V1 undergo differential maturation after eye opening (Kuhlman et al., 2011; Li et al., 2012). For example, the PC gradually sharpens its orientation tuning (Li et al., 2012), while the PV cells gradually lose their initial orientation bias from eye opening to the CP onset (Kuhlman et al., 2011; Li et al., 2012). Our observation of selective, target-cell-independent modulation of STD at intracortical excitatory synapses in the developing layer 4 circuit is largely in line with these changes in visual response properties during the development. The experience-dependent reduction of basal transmission and STD of layer 4 PC→PC synapses during this period favors a sharpening of orientation tuning and more reliable responses to rhythmic visual inputs in visual cortical PCs (Ko et al., 2013). Moreover, the reduced STD at cortical PC→PV synapses at the CP onset (Figures 2A–2C) could enhance the excitatory drive to the PV cell and facilitate the recruitment of PV cells upon visual inputs. The recruitment of activated cortical PV cells has been shown to effectively suppress cortical spontaneous activity originating from the visual thalamus (Toyoizumi et al., 2013) and to enhance the processing of nature scenes in the mouse V1 (Zhu et al., 2015). Meanwhile, cortical Sst cells also play important roles in processing sensory information (Melamed et al., 2008; Wilson et al., 2012; Lee et al., 2014; Petersen, 2014; Chen et al., 2015). In the mouse V1, they show similar orientation and direction selectivity as that of PCs, exhibiting tuning from weakly tuned to highly selective (Ma et al., 2010). However, it needs further studies, using in vivo imaging guided recording, to address how synaptic functional changes in cortical Sst cells and other distinct changes in the layer 4 synaptic circuit before the CP contribute to the development of their tuning properties.

Functional maturation of cortical excitatory and inhibitory networks is important for gating the emergence of experience-dependent CP plasticity (Toyoizumi et al., 2013) and visual functions (Griffen et al., 2012) in developing V1. In addition to the well-known inhibitory threshold mechanism, the experience-dependent, target cell-independent modulation of synaptic dynamics we observed at distinct intracortical excitatory synapses may represent another essential circuit mechanism for regulating the CP opening.

EXPERIMENTAL PROCEDURES

Animals

Wild-type C57BL/6 mice and four transgenic lines—*B13* (*PV-EGFP*, J. Z. Huang, CSHL; Dumitriu et al., 2007), *PV-IRES-Cre* (Jax No.: 8069, generated by S. Arbor, FMI), *Sst-IRES-Cre* (J. Z. Huang, CSHL; Jax no. 13044), and the tdTomato reporter *Ai9* (*Rosa-CAG-LSL- tdTomato-WPRE*; H-k Zeng, Allen Brain Institute; Jax No. 7909) (Madisen et al., 2010)—were used in the present study. The *PV-IRES-Cre* and *Sst-IRES-Cre* mice were crossed to the *Ai9* mice to generate *PV-Cre::Ai9* and *Sst-Cre::Ai9* alleles, in which most PV and Sst cells are genetically labeled by red fluorescence protein tdTomato, respectively. All pups were reared in a normal 12/12 hr light/dark cycle, except those reared in the homemade dark cages from birth. The protocols of mouse breeding, care, and experimentation were approved by the Animal Care and Use Committees of the State Key Laboratory of Cognitive Neuroscience and Learning at Beijing Normal University (IACUC-BNU-NKLCNL-2013-10) and Shanghai Institute for Biological Sciences, Chinese Academy of Sciences (Ref. NO. NA-100418).

Preparation of Brain Slices

The preparation of visual cortical slices from young mice at the designed postnatal days followed a method described in our previous studies (Lu et al., 2007; Zhang et al., 2009). In brief, *WT*, *B13*, *PV-Cre::Ai9*, or *Sst-Cre::Ai9* mice at P14–31 were anaesthetized with sodium pentobarbital (Nembutal, Abott, 50 mg/kg, intraperitoneally [i.p.]). After decapitation, the brain was dissected rapidly and placed in ice-cold oxygenated aCSF containing 125mM NaCl, 3 mM KCl, 2 mM $CaCl_2$, 2 mM $MgSO_4$, 1.25 mM NaH_2PO_4, 1.3 Na^+-ascorbate, 0.6 Na^+-pyruvate, 26 $NaHCO_3$, and 11 glucose (pH 7.4). For dark-reared animals, the above procedures were completed in red-lighting dark room. Coronal section slices (300–350 μm thick) were made with a vibratome (Vibratome or VT-1200S, Leica) and incubated in a chamber with oxygenated aCSF at 34°C for 30 min and then at room temperature (20°C –25°C) for > 30 min before the use for recording experiments.

Electrophysiology

The cortical slices in the recording chamber were perfused with oxygenated aCSF at a rate of 2 ml/min. Whole-cell recordings, in either voltage- or current-clamp mode, were made from pairs of excitatory PCs, GABAergic PV or Sst cells in the visual cortical layer 4, under an Olympus microscope (BX51WI) equipped with an infrared video camera (IR-1000) and differential interference contrast optics. The borosilicate glass microelectrodes were pulled by a Sutter puller (P97 or P-1000) and was filled with an internal solution containing 130 mM K^+-gluconate, 20 mM KCl, 10 mM HEPES, 0.2 mM EGTA, 4 mM Mg_2ATP, 0.3 mM Na_2GTP, and 10 mM Na_2-phosphocreatine (at pH 7.3, 290–310 mOsm) for recording excitatory postsynaptic currents or potentials (EPSCs or EPSPs), or with a high-Cl^- solution containing 94 mM K-gluconate, 60 mM KCl, 10 mM HEPES, 0.2 mM EGTA, 4 mM Mg_2ATP, 0.3 mM Na_2GTP, and 10 mM Na_2-phosphocreatine (at pH 7.3, 290–310 mOsm) for recording inhibitory postsynaptic responses. The micropipette resistance was 2–4 MΩ. To assay the efficacy and dynamics of unitary synaptic transmission, a train of 5 or 10 current pulses (2 ms duration, 0.8–2 nA at 20 or 40 Hz) was intracellularly injected to the presynaptic neuron (in the current-clamp mode) at time intervals of 10 or 20 s. For activating long-range TC synapses on layer 4 cells, similar trains of 5 pulses (at 20 Hz) were delivered through a concentric tungsten electrode (125 μm outer diameter [o.d.]) placed in the white matter layer, and stimulation intensity was set at a magnitude of ~20% above the threshold values. Evoked postsynaptic potentials or currents (PSPs/PSCs) were recorded from postsynaptic neuron (in the current-clamp mode) with an Axopatch-700B amplifier (Molecular Devices). In recordings from the postsynaptic PV cell, due to its small membrane resistance (~60 MΩ), series resistance (R_s) compensation was essential in the voltage-clamp mode. However, because the R_s compensation could bring about two potential pitfalls, adding noise to the current measurement and easy prone to membrane oscillations, PSPs, rather than PSCs, were recorded from the PV cell under the current-clamp, using the bridge-balance to compensate the R_s-induced voltage drop. Short-term synaptic dynamics measured in the two modes showed similar magnitudes and temporal properties (Figure S1). To isolate tcEPSPs, a cortical silencing cocktail of muscimol (50 μM, a $GABA_A$ receptor agonist) and SCH50911 (70 μM, a $GABA_B$ receptor antagonist) was applied in the aCSF solution, following a method described in previous studies (Liu et al., 2007; Khibnik et al., 2010). All recordings were done at the temperature of 31°C–33°C (Warner Instrument Corporation, TC-324B). Individual synaptic responses with the amplitude below the noise level were identified as the failure and included in the calculation of mean PSPs/PSCs as events with the amplitude of 0. Values of R_s of postsynaptic neuron were monitored throughout the recording. Synaptic responses were accepted for analysis only for the cases, in which the recorded neurons showed resting membrane potentials < −60 mV, access resistance (R_a) < 30 MΩ, and the R_s change < 30% throughout the experiment. Electric signals were filtered at 2 or 4 kHz (low pass), digitized by a Digidata 1322A converter board (Molecular Devices) and acquired at 20 KHz with the pClamp9.2/10 (Molecular Devices) into a computer for further analysis with custom programs in the MATLAB (MathWorks). All chemicals were obtained from Sigma-Aldrich or Tocris Bioscience.

Data Analysis

In the present study, 255 mice in total were used, and the data for each condition were collected from slices obtained from at least 3 mice. Data from recorded cells showing R_a > 30 MΩ were excluded from calculating the synaptic strength, but were included in calculating the connection probability and STP. The amplitudes of the first averaged PSP/PSC elicited by the train stimuli were used for assaying the basal synaptic strength, while the C.V. of basal transmission was calculated from the amplitudes of individual trials. The rise time of PSCs/PSPs was calculated from 10% to 90% rising phase, and the decay time constant (τ_{decay}) was estimated by using a single exponential fit to the decay phase from the peak to 20% of amplitudes. To assay the efficacy of electrical synapse between two cortical PV cells, averaged values of the two unidirectional-coupling index, which is a ratio of the membrane deflection amplitude in one cell and that of the other connected cell elicited by hyperpolarizing current injection (200–350 pA, 300 ms), was used. The variance-mean analysis was carried out on synaptic responses (mainly EPSCs) evoked by the presynaptic pulse trains. The PSC amplitude was determined for each pulse, and the mean (M) and variance (V) were plotted against each other. Synaptic quantal parameters including number of release sites (N) and quantal size (Q) were obtained by fitting the relationship between M and V to the parabola: $V = QM - M^2/N$ (Scheuss and Neher, 2001; Gu et al., 2013). As under the condition of absence of non-linear summation of small EPSPs, the V-M analysis is also be valid for PSPs (Scheuss and Neher, 2001). We considered only those cases in which the R^2 value of the fit was >0.33 and estimated N was <50.

Statistical Analysis

All data are presented as mean ± SEM, unless otherwise noted. For comparisons between two conditions, the statistical significance (p) values were obtained using unpaired two-tailed Student's t test when the data were in the normal distribution (tested by the Jarque-Bera test). For data showing the non-normal distribution, the nonparametric Kolmogorov-Smirnov and the paired-sample sign tests were used. The chi-square (χ^2) test was used to determine the significance of the connectivity difference between different developmental stages. The comparison of short-term plasticity between different developmental stages was done by ANOVA.

SUPPLEMENTAL INFORMATION

Supplemental Information includes two figures and two tables and can be found with this article online at http://dx.doi.org/10.1016/j.celrep.2016.07.013.

AUTHOR CONTRIBUTIONS

Q.M. and L.Y. performed electrophysiology experiments. Q.M., L.Y., and M.J.R. analyzed the data. Q.Y. and X.L. helped the immune-staining of cortical interneurons. X.Z. and Q.M. designed the experiments and wrote the manuscript.

ACKNOWLEDGMENTS

The authors wish to thank Dr. J.Z. Huang (CSHL) for providing the *B13* mice and Drs. Y.X. Lin (MIT) and H.W. Tao (USC) for their comments on the

Please cite this article in press as: Miao et al., Selective Maturation of Temporal Dynamics of Intracortical Excitatory Transmission at the Critical Period Onset, Cell Reports (2016), http://dx.doi.org/10.1016/j.celrep.2016.07.013

manuscript. This work was supported by a grant from the State Key Research Program of China (2011CBA00403) (to X.Z.).

Received: October 28, 2015
Revised: May 10, 2016
Accepted: July 1, 2016
Published: July 28, 2016

REFERENCES

Abbott, L.F., and Regehr, W.G. (2004). Synaptic computation. Nature *431*, 796–803.

Ahmed, B., Anderson, J.C., Martin, K.A., and Nelson, J.C. (1997). Map of the synapses onto layer 4 basket cells of the primary visual cortex of the cat. J. Comp. Neurol. *380*, 230–242.

Bartley, A.F., Huang, Z.J., Huber, K.M., and Gibson, J.R. (2008). Differential activity-dependent, homeostatic plasticity of two neocortical inhibitory circuits. J. Neurophysiol. *100*, 1983–1994.

Beierlein, M., and Connors, B.W. (2002). Short-term dynamics of thalamocortical and intracortical synapses onto layer 6 neurons in neocortex. J. Neurophysiol. *88*, 1924–1932.

Beierlein, M., Gibson, J.R., and Connors, B.W. (2003). Two dynamically distinct inhibitory networks in layer 4 of the neocortex. J. Neurophysiol. *90*, 2987–3000.

Blue, M.E., and Parnavelas, J.G. (1983). The formation and maturation of synapses in the visual cortex of the rat. II. Quantitative analysis. J. Neurocytol. *12*, 697–712.

Chattopadhyaya, B., Di Cristo, G., Higashiyama, H., Knott, G.W., Kuhlman, S.J., Welker, E., and Huang, Z.J. (2004). Experience and activity-dependent maturation of perisomatic GABAergic innervation in primary visual cortex during a postnatal critical period. J. Neurosci. *24*, 9598–9611.

Chen, H.X., and Roper, S.N. (2004). Tonic activity of metabotropic glutamate receptors is involved in developmental modification of short-term plasticity in the neocortex. J. Neurophysiol. *92*, 838–844.

Chen, G., Rasch, M.J., Wang, R., and Zhang, X.H. (2015). Experience-dependent emergence of beta and gamma band oscillations in the primary visual cortex during the critical period. Sci. Rep. *5*, 17847.

Choi, S.Y., Morales, B., Lee, H.K., and Kirkwood, A. (2002). Absence of long-term depression in the visual cortex of glutamic Acid decarboxylase-65 knockout mice. J. Neurosci. *22*, 5271–5276.

Clement, J.P., Ozkan, E.D., Aceti, M., Miller, C.A., and Rumbaugh, G. (2013). SYNGAP1 links the maturation rate of excitatory synapses to the duration of critical-period synaptic plasticity. J. Neurosci. *33*, 10447–10452.

Corlew, R., Wang, Y., Ghermazien, H., Erisir, A., and Philpot, B.D. (2007). Developmental switch in the contribution of presynaptic and postsynaptic NMDA receptors to long-term depression. J. Neurosci. *27*, 9835–9845.

Cruikshank, S.J., Urabe, H., Nurmikko, A.V., and Connors, B.W. (2010). Pathway-specific feedforward circuits between thalamus and neocortex revealed by selective optical stimulation of axons. Neuron *65*, 230–245.

Dumitriu, D., Cossart, R., Huang, J., and Yuste, R. (2007). Correlation between axonal morphologies and synaptic input kinetics of interneurons from mouse visual cortex. Cereb. Cortex *17*, 81–91.

Espinosa, J.S., and Stryker, M.P. (2012). Development and plasticity of the primary visual cortex. Neuron *75*, 230–249.

Etherington, S.J., and Williams, S.R. (2011). Postnatal development of intrinsic and synaptic properties transforms signaling in the layer 5 excitatory neural network of the visual cortex. J. Neurosci. *31*, 9526–9537.

Fino, E., and Yuste, R. (2011). Dense inhibitory connectivity in neocortex. Neuron *69*, 1188–1203.

Gibson, J.R., Beierlein, M., and Connors, B.W. (1999). Two networks of electrically coupled inhibitory neurons in neocortex. Nature *402*, 75–79.

Gordon, J.A., and Stryker, M.P. (1996). Experience-dependent plasticity of binocular responses in the primary visual cortex of the mouse. J. Neurosci. *16*, 3274–3286.

Griffen, T.C., Wang, L., Fontanini, A., and Maffei, A. (2012). Developmental regulation of spatio-temporal patterns of cortical circuit activation. Front. Cell. Neurosci. *6*, 65.

Gu, Y., Huang, S., Chang, M.C., Worley, P., Kirkwood, A., and Quinlan, E.M. (2013). Obligatory role for the immediate early gene NARP in critical period plasticity. Neuron *79*, 335–346.

Gupta, A., Wang, Y., and Markram, H. (2000). Organizing principles for a diversity of GABAergic interneurons and synapses in the neocortex. Science *287*, 273–278.

He, L.J., Liu, N., Cheng, T.L., Chen, X.J., Li, Y.D., Shu, Y.S., Qiu, Z.L., and Zhang, X.H. (2014). Conditional deletion of Mecp2 in parvalbumin-expressing GABAergic cells results in the absence of critical period plasticity. Nat. Commun. *5*, 5036.

Hensch, T.K. (2004). Critical period regulation. Annu. Rev. Neurosci. *27*, 549–579.

Hensch, T.K. (2005). Critical period plasticity in local cortical circuits. Nat. Rev. Neurosci. *6*, 877–888.

Hensch, T.K., Fagiolini, M., Mataga, N., Stryker, M.P., Baekkeskov, S., and Kash, S.F. (1998). Local GABA circuit control of experience-dependent plasticity in developing visual cortex. Science *282*, 1504–1508.

Hu, H., Ma, Y., and Agmon, A. (2011). Submillisecond firing synchrony between different subtypes of cortical interneurons connected chemically but not electrically. J. Neurosci. *31*, 3351–3361.

Hubel, D.H., and Wiesel, T.N. (1970). The period of susceptibility to the physiological effects of unilateral eye closure in kittens. J. Physiol. *206*, 419–436.

Jiang, B., Sohya, K., Sarihi, A., Yanagawa, Y., and Tsumoto, T. (2010). Laminar-specific maturation of GABAergic transmission and susceptibility to visual deprivation are related to endocannabinoid sensitivity in mouse visual cortex. J. Neurosci. *30*, 14261–14272.

Khibnik, L.A., Cho, K.K., and Bear, M.F. (2010). Relative contribution of feedforward excitatory connections to expression of ocular dominance plasticity in layer 4 of visual cortex. Neuron *66*, 493–500.

Kloc, M., and Maffei, A. (2014). Target-specific properties of thalamocortical synapses onto layer 4 of mouse primary visual cortex. J. Neurosci. *34*, 15455–15465.

Klug, A., Borst, J.G.G., Carlson, B.A., Kopp-Scheinpflug, C., Klyachko, V.A., and Xu-Friedman, M.A. (2012). How do short-term changes at synapses fine-tune information processing? J. Neurosci. *32*, 14058–14063.

Klyachko, V.A., and Stevens, C.F. (2006). Excitatory and feed-forward inhibitory hippocampal synapses work synergistically as an adaptive filter of natural spike trains. PLoS Biol. *4*, e207.

Ko, H., Cossell, L., Baragli, C., Antolik, J., Clopath, C., Hofer, S.B., and Mrsic-Flogel, T.D. (2013). The emergence of functional microcircuits in visual cortex. Nature *496*, 96–100.

Kuhlman, S.J., Tring, E., and Trachtenberg, J.T. (2011). Fast-spiking interneurons have an initial orientation bias that is lost with vision. Nat. Neurosci. *14*, 1121–1123.

Kuhlman, S.J., Olivas, N.D., Tring, E., Ikrar, T., Xu, X., and Trachtenberg, J.T. (2013). A disinhibitory microcircuit initiates critical-period plasticity in the visual cortex. Nature *501*, 543–546.

Larsen, R.S., Corlew, R.J., Henson, M.A., Roberts, A.C., Mishina, M., Watanabe, M., Lipton, S.A., Nakanishi, N., Pérez-Otaño, I., Weinberg, R.J., and Philpot, B.D. (2011). NR3A-containing NMDARs promote neurotransmitter release and spike timing-dependent plasticity. Nat. Neurosci. *14*, 338–344.

Leal, K., Mochida, S., Scheuer, T., and Catterall, W.A. (2012). Fine-tuning synaptic plasticity by modulation of Ca(V)2.1 channels with Ca2+ sensor proteins. Proc. Natl. Acad. Sci. USA *109*, 17069–17074.

Lee, S.H., Kwan, A.C., and Dan, Y. (2014). Interneuron subtypes and orientation tuning. Nature *508*, E1–E2.

Levelt, C.N., and Hübener, M. (2012). Critical-period plasticity in the visual cortex. Annu. Rev. Neurosci. *35*, 309–330.

Li, Y.T., Ma, W.P., Pan, C.J., Zhang, L.I., and Tao, H.W. (2012). Broadening of cortical inhibition mediates developmental sharpening of orientation selectivity. J. Neurosci. *32*, 3981–3991.

Liu, B.H., Wu, G.K., Arbuckle, R., Tao, H.W., and Zhang, L.I. (2007). Defining cortical frequency tuning with recurrent excitatory circuitry. Nat. Neurosci. *10*, 1594–1600.

Lu, J.T., Li, C.Y., Zhao, J.P., Poo, M.M., and Zhang, X.H. (2007). Spike-timing-dependent plasticity of neocortical excitatory synapses on inhibitory interneurons depends on target cell type. J. Neurosci. *27*, 9711–9720.

Lu, J., Tucciarone, J., Lin, Y., and Huang, Z.J. (2014). Input-specific maturation of synaptic dynamics of parvalbumin interneurons in primary visual cortex. Proc. Natl. Acad. Sci. USA *111*, 16895–16900.

Ma, W.P., Liu, B.H., Li, Y.T., Huang, Z.J., Zhang, L.I., and Tao, H.W. (2010). Visual representations by cortical somatostatin inhibitory neurons–selective but with weak and delayed responses. J. Neurosci. *30*, 14371–14379.

Ma, Y., Hu, H., and Agmon, A. (2012). Short-term plasticity of unitary inhibitory-to-inhibitory synapses depends on the presynaptic interneuron subtype. J. Neurosci. *32*, 983–988.

Madisen, L., Zwingman, T.A., Sunkin, S.M., Oh, S.W., Zariwala, H.A., Gu, H., Ng, L.L., Palmiter, R.D., Hawrylycz, M.J., Jones, A.R., et al. (2010). A robust and high-throughput Cre reporting and characterization system for the whole mouse brain. Nat. Neurosci. *13*, 133–140.

Maffei, A., Nelson, S.B., and Turrigiano, G.G. (2004). Selective reconfiguration of layer 4 visual cortical circuitry by visual deprivation. Nat. Neurosci. *7*, 1353–1359.

Markram, H., Wang, Y., and Tsodyks, M. (1998). Differential signaling via the same axon of neocortical pyramidal neurons. Proc. Natl. Acad. Sci. USA *95*, 5323–5328.

Markram, H., Toledo-Rodriguez, M., Wang, Y., Gupta, A., Silberberg, G., and Wu, C. (2004). Interneurons of the neocortical inhibitory system. Nat. Rev. Neurosci. *5*, 793–807.

Mataga, N., Mizuguchi, Y., and Hensch, T.K. (2004). Experience-dependent pruning of dendritic spines in visual cortex by tissue plasminogen activator. Neuron *44*, 1031–1041.

Melamed, O., Barak, O., Silberberg, G., Markram, H., and Tsodyks, M. (2008). Slow oscillations in neural networks with facilitating synapses. J. Comput. Neurosci. *25*, 308–316.

Mitra, A., Mitra, S.S., and Tsien, R.W. (2012). Heterogeneous reallocation of presynaptic efficacy in recurrent excitatory circuits adapting to inactivity. Nat. Neurosci. *15*, 250–257.

Pangratz-Fuehrer, S., and Hestrin, S. (2011). Synaptogenesis of electrical and GABAergic synapses of fast-spiking inhibitory neurons in the neocortex. J. Neurosci. *31*, 10767–10775.

Petersen, C.Ch. (2014). Cell-type specific function of GABAergic neurons in layers 2 and 3 of mouse barrel cortex. Curr. Opin. Neurobiol. *26*, 1–6.

Pfeffer, C.K., Xue, M., He, M., Huang, Z.J., and Scanziani, M. (2013). Inhibition of inhibition in visual cortex: the logic of connections between molecularly distinct interneurons. Nat. Neurosci. *16*, 1068–1076.

Postma, F., Liu, C.H., Dietsche, C., Khan, M., Lee, H.K., Paul, D., and Kanold, P.O. (2011). Electrical synapses formed by connexin36 regulate inhibition- and experience-dependent plasticity. Proc. Natl. Acad. Sci. USA *108*, 13770–13775.

Pouille, F., and Scanziani, M. (2001). Enforcement of temporal fidelity in pyramidal cells by somatic feed-forward inhibition. Science *293*, 1159–1163.

Reyes, A., Lujan, R., Rozov, A., Burnashev, N., Somogyi, P., and Sakmann, B. (1998). Target-cell-specific facilitation and depression in neocortical circuits. Nat. Neurosci. *1*, 279–285.

Rotman, Z., Deng, P.Y., and Klyachko, V.A. (2011). Short-term plasticity optimizes synaptic information transmission. J. Neurosci. *31*, 14800–14809.

Rozov, A., and Burnashev, N. (1999). Polyamine-dependent facilitation of postsynaptic AMPA receptors counteracts paired-pulse depression. Nature *401*, 594–598.

Rudy, B., Fishell, G., Lee, S., and Hjerling-Leffler, J. (2011). Three groups of interneurons account for nearly 100% of neocortical GABAergic neurons. Dev. Neurobiol. *71*, 45–61.

Scheuss, V., and Neher, E. (2001). Estimating synaptic parameters from mean, variance, and covariance in trains of synaptic responses. Biophys. J. *81*, 1970–1989.

Takesian, A.E., Kotak, V.C., and Sanes, D.H. (2010). Presynaptic $GABA_{(B)}$ receptors regulate experience-dependent development of inhibitory short-term plasticity. J. Neurosci. *30*, 2716–2727.

Takesian, A.E., Kotak, V.C., Sharma, N., and Sanes, D.H. (2013). Hearing loss differentially affects thalamic drive to two cortical interneuron subtypes. J. Neurophysiol. *110*, 999–1008.

Thomson, A.M. (1997). Activity-dependent properties of synaptic transmission at two classes of connections made by rat neocortical pyramidal axons in vitro. J. Physiol. *502*, 131–147.

Toyoizumi, T., Miyamoto, H., Yazaki-Sugiyama, Y., Atapour, N., Hensch, T.K., and Miller, K.D. (2013). A theory of the transition to critical period plasticity: inhibition selectively suppresses spontaneous activity. Neuron *80*, 51–63.

Wang, B.S., Sarnaik, R., and Cang, J. (2010). Critical period plasticity matches binocular orientation preference in the visual cortex. Neuron *65*, 246–256.

Wang, L., Fontanini, A., and Maffei, A. (2012). Experience-dependent switch in sign and mechanisms for plasticity in layer 4 of primary visual cortex. J. Neurosci. *32*, 10562–10573.

Wilson, N.R., Runyan, C.A., Wang, F.L., and Sur, M. (2012). Division and subtraction by distinct cortical inhibitory networks in vivo. Nature *488*, 343–348.

Wyatt, R.M., Tring, E., and Trachtenberg, J.T. (2012). Pattern and not magnitude of neural activity determines dendritic spine stability in awake mice. Nat. Neurosci. *15*, 949–951.

Xu, X., Roby, K.D., and Callaway, E.M. (2010). Immunochemical characterization of inhibitory mouse cortical neurons: three chemically distinct classes of inhibitory cells. J. Comp. Neurol. *518*, 389–404.

Xu, H., Jeong, H.Y., Tremblay, R., and Rudy, B. (2013). Neocortical somatostatin-expressing GABAergic interneurons disinhibit the thalamorecipient layer 4. Neuron *77*, 155–167.

Zhang, S.Y., Xu, M., Miao, Q.L., Poo, M.M., and Zhang, X.H. (2009). Endocannabinoid-dependent homeostatic regulation of inhibitory synapses by miniature excitatory synaptic activities. J. Neurosci. *29*, 13222–13231.

Zhu, Y., Qiao, W., Liu, K., Zhong, H., and Yao, H. (2015). Control of response reliability by parvalbumin-expressing interneurons in visual cortex. Nat. Commun. *6*, 6802.